IEEE NPSS (Toronto), UOIT, Oshawa, ON, 25 & 26 June, 2010
International Workshop on Real Time Measurement, Instrumentation & Control [RTMIC]

Depth profiling of radiological contamination in sand using Principal Component Analysis

Jamie C. Adams [1], Matthew Mellor [2] & Malcolm J. Joyce [1]

[1] Engineering Department, Lancaster University, Lancaster. LA1 4YR. UK
[2] REACT Engineering Ltd, Fleswick Court, Westlakes Science and Technology Park, Moor Row, Whitehaven, Cumbria. CA24 3HZ. UK

***Abstract*—The depth of a caesium-137 radioactive source buried in sand has been determined using Principal Component Analysis. A bespoke phantom filled with fine-grade silica sand has been used. The source was placed in the sand at depths of between 5 to 50mm, using a calibrated source slider. At each depth, γ-ray spectra were recorded at an external face of the phantom using a cadmium telluride γ-ray detector. A model was then developed relating the depth to the output of the Principle Component Analysis. Two principal component vectors have been extracted for each depth spectrum. The angle (θ) between these at each depth is used to derive a function of depth.**

I. INTRODUCTION

The contamination of land by radioactive material often plagues old nuclear facilities and surrounding areas. This is because the land in which it is buried partially shields the radiation emitted by the contamination, complicating the ease with which it is located and assessed. Several techniques have been developed to identify the location of contamination on the surface in 2-dimensions, when shielded by another material. A recently-established technique is the N-Visage™ system, developed by REACT Engineering Ltd [1]. This system is able to accurately infer source location in 2-dimensions above shielding, but thus far has not been able to infer depth. Where contamination has accrued over several decades, and is in an environment where the land is essentially unlimited in scope, the limits on the likely depth of the contamination can be very significant, indirectly implying significant uncertainty in the extent of radioactivity present.

Several techniques have been explored to indicate the depth of contamination in recent years, including the *linear attenuation method* in which the relative differences in attenuation of the x-ray and γ-ray in, for example, the caesium-137 spectrum are exploited to infer the depth [2]. However, this is limited to the depth at which the x-ray is completely attenuated away, ~20mm, which is rarely sufficient for industrial applications, where the contamination can be significantly deeper. In this paper a new approach to inferring the depth of contamination in land is introduced in which Principle Component Analysis (PCA) has been used to extract trends in the shielding effect of the land on the generic structure of the γ-ray response of a semi-conductor detector. This enables a related angle to be derived which has direct correspondence with the contamination depth.

II. METHODS

A. *Principal Component Analysis (PCA)*

PCA has been used in a broad range of different fields, for example in facial recognition, environmental science and biological applications. PCA can be used to summarize variance in multi-dimension datasets, such as γ-spectra. In multi-dimension datasets correlations between dimensions can often be seen; in the case of a γ-spectrum, for example, if one bin contains a large number of counts, it is likely that the immediately adjacent bins will as well. When this is observed, it may be possible to reduce the dimension of a dataset without losing information by capturing these correlations. PCA is the simplest method for data reduction; it is a quantitative, linear method for simplifying the data by representing it as a sum of a smaller number of 'Principle Components' (PCs). PCA finds the optimal set of PC's such that each PC is orthogonal to all others in the set, and such that the a data reduction to dimension N is optimal in the sense that the sum-of-squares error between the dimension-reduced and original data is the smallest that can be achieved with a linear, N-dimensional representation. It is usual for the first few PCs to explain the majority of the original dataset; in this case the lost information is often noise. A comprehensive review of PCA can be found in [3].

B. Experimental design

In this research a bespoke sand phantom, previously developed for another project [4] was used. The phantom was filled to a depth of 0.26m using fine-grade silica sand. The phantom consists of a modified tank, constructed out of acrylic glass (polymethylmethacrylate (PMM)); this material was used to minimize photon scatter by the phantom itself. A rectangular chamber runs through the middle of the phantom (along the horizontal plane). A calibrated plastic slider passes through the length of this chamber. The slider has depth increments of 1mm ± 0.5mm marked off, calibrated using trigonometry. The slider is designed to enable a small radiological disc source (radius=25mm, depth=2mm) to be held securely in place at a specified depth ranging from between 5 to 50mm. This is achieved as the phantom has a sloping front face, with one end being shallower compared to the other. The depth is varied along the horizontal plane, and was tracked by moving the γ-detector parallel with the source, along the external, front face of the phantom.

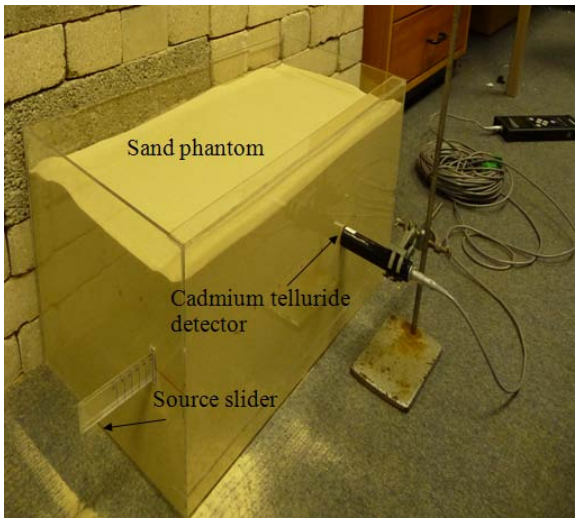

Fig. 1. The sand phantom used in this research.

In this research a caesium-137 disc source, with a calibrated activity of 382 kBq was positioned under different depths of sand at increments of 1 mm ± 0.5 mm. By gathering spectra for 300s at each different depth, a model was generated for depths between 5 to 50mm. In this arrangement the detector was positioned flush, against the external face of the phantom, pointing towards the source. The detector was moved to be parallel and at the same height to the source for all depth measurements ± 0.5mm. The experimental setup can be seen in fig. 1.

C. Radiation detection

Owing to its robust and compact design, an ICS-4000e Radionuclide Identifier was used in conjunction with an XP Submersible Gamma Ray Probe (XRF Corporation, Woburn, MA) [5]. The system is an integrated unit with a 10 x 10 x 1mm cadmium telluride (CdTe) detector; the generated spectra are first uploaded onto a handheld storage device, before being transferred to a PC. The CdTe detector also offers superior energy resolution when compared to sodium iodide (NaI).

D. Calculating scatter and Compton energies for a caesium-137 source

The structure of a γ-ray spectrum at energies lower than the photopeak(s) arises from photons that have undergone Compton scattering out of the detector, and only leave part of the total energy of the photon in the detector.

We distinguish between two types of external scattering event; those which happen within the matrix medium between the source and the detector, and those which happen within the casing and electronics surrounding the detector. The former are potentially useful as the implicitly carry information about the matrix; the latter are not of interest in the present study.

The backscatter peak is the spectral feature that corresponds to photons that have been scattered through 180° in material immediately behind the detector before then being detected; this is the lowest energy that can be recorded for a photon undergoing a single Compton interaction outside the detector, and then interacting with the detector by the photoelectric effect.

The backscattered photon energy, E_γ', is given in (1):

$$E_\gamma' = E_\gamma \left\{ \frac{1}{\left(1 + E_\gamma \left[1 - \cos\theta\right] / m_o c^2\right)} \right\} \quad (1)$$

where, E_γ is the full energy γ-ray (keV), θ is the scattering angle (°) and $m_o c^2$ is the rest mass energy of an electron (0.511 keV). In this example E_γ = 661.7 keV and the angle (θ) is 180°, this results in maximum energy dissipation as the γ-ray travels backwards. This gives a maximum backscatter value of 184.3 keV. For a more detailed discussion see [6].

The Compton shelf arises when a photon interacts with the detector by Compton scattering and then the

scattered photon escapes. There is a maximum possible energy transfer to the detector associated with this event, corresponding to the case where the scattering angle is 180°. This energy value was calculated using (2),

$$E_e = E_\gamma - E_\gamma' \qquad (2)$$

where E_e is the recoil electron, E_γ is the γ-ray and E_γ' is the scattered γ-ray. In this case E_γ = 661.7 keV and E_γ' = 184.3 keV (the maximum backscatter energy). This results in Compton energy (E_e) of 477.4 keV.

A region of interest covering the 661.7 keV γ-ray photopeak was also used in this research. This was read directly from the spectrum taken for each depth setting. A region of interest (ROI) was used to capture the full extent of the 661.7 keV photopeak. The calculated energy for the maximum backscattered photon and the Compton shelf are in agreement with observed values, shown in fig. 2(a). It is known that, as the depth of shielding increases between a γ-emitting source and a detector, the full energy γ-ray will become more attenuated. Fig. 2(a) shows the γ-ray spectra for two depth experiments (only the two depth spectra for 5mm and 50mm have been plotted for clarity). Fig. 2(b) is a plot of total count rate versus depth which demonstrates how the total count rate falls exponentially with increased shielding depth. To correct for this change in total count rate (as each depth experiment was conducted for 300s), each separate spectra has been normalised to its total count. The resulting normalized graph for all depth spectra can be seen in fig. 3.

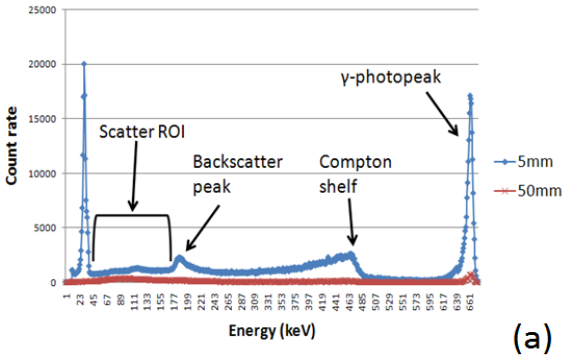

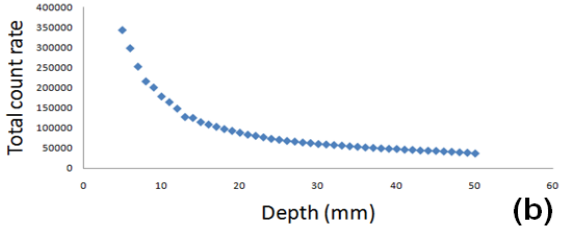

Fig. 2(a). The γ-ray spectra from the CdTe detector. For clarity only the data for two most extreme depth experiments of 5mm and 50mm are presented. 2(b) The total count rate for each depth experiment.

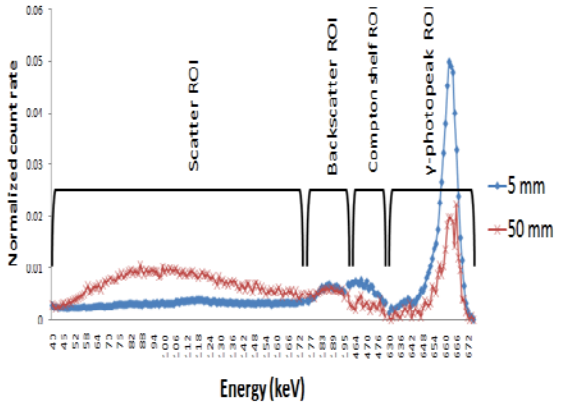

Fig. 3. A plot of the normalized count rate vs. energy for the 5mm and 50mm depth experiments. Only the four spectral features being discussed in this paper have been identified.

III. RESULTS

A. Scatter, backscatter, Compton shelf and γ-photopeak analysis

Fig. 3 displays the count-normalized spectra for the 5mm and 50mm depth experiments. Not surprisingly, pattern of increasing scatter and decreasing γ-photopeak was seen as the depth of shielding increases. The normalized count rates for energies between 40keV to 174keV were summed to give a summed ROI for the *scatter part* of each spectrum. The same summation was carried out for energies between 630keV to 675keV, covering the γ-photopeak. A ROI was also established using the summed count rates for the backscatter peak taking energies between 175keV and 195keV and for the *Compton shelf* using 460keV to 480keV. Fig. 4 displays a plot of the summed value for each of these four spectral ROIs, for each depth experiment. Very little variation is seen as depth increases for both the backscatter peak and the Compton shelf. However, a relationship appears to exist linking the scatter and the γ-photopeak, as might be expected intuitively. To study these relationships further, and to see how they vary with depth, PCA was conducted.

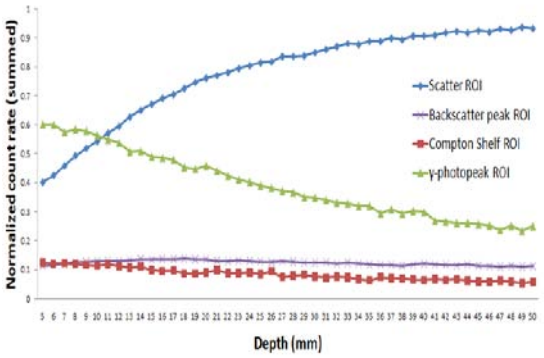

Fig.4. A plot of the summed, normalized count rates for the scatter ROI, backscatter ROI, Compton shelf ROI and γ-photopeak ROI for each depth experiment.

B. PCA models

For comparison three separate sets of spectral data were modeled using PCA, these were: (model A) the scatter and γ-photopeak ROIs; (model B) the scatter, backscatter, Compton shelf and γ-photopeak ROIs and finally (model C) the complete spectrum for each depth experiment. Fig. 5 is a plot for each of these PCA models. All three models give a high percentage for variability explained by the first principal component (PC). All three models have a first PC of 83% with the second PC explaining a further 10% of the data. Only PC1 and PC2 are used in the subsequent analysis, due to the significant values these have in explaining the total variability of the dataset.

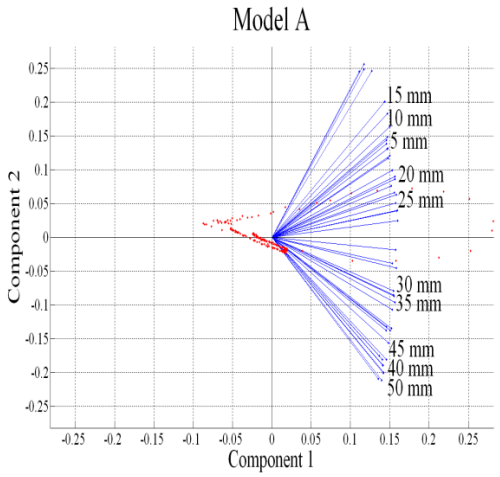

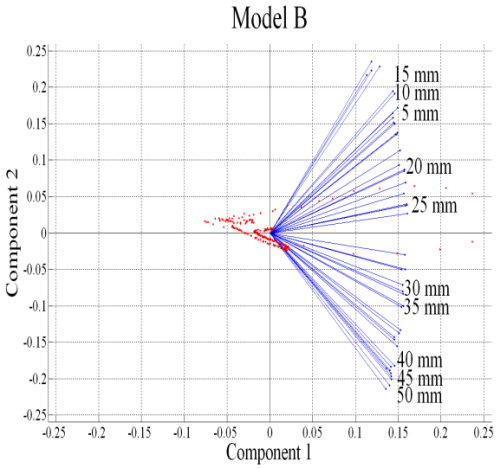

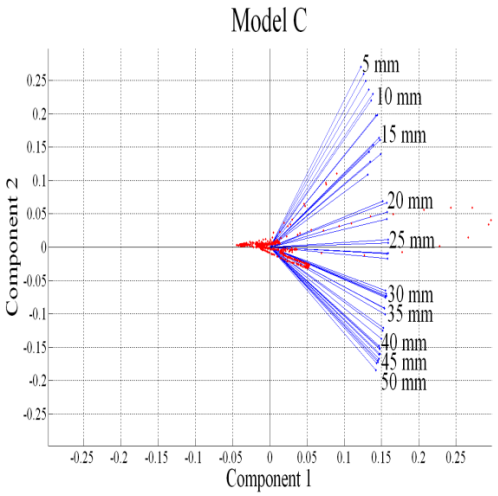

Fig. 5. PCA results taken from: the scatter and γ-photopeak ROIs (model A); the scatter, backscatter, Compton shelf and γ-photopeak ROIs (model B) and finally the complete γ-ray spectrum (model C). All 46 depth experiments (5 to 50mm) were used for each model. For clarity only every fifth depth experiment has been labeled.

The plots in fig. 5 were generated by plotting the first two PC coefficient vectors (loadings) by the first two columns of the original spectra in the new coordinate system defined by the PCs. Each line represents a vector for each depth experiment. The length and direction of each indicates how each vector contributes to PC1 and PC2. The points indicate each energy count and their locations relate that energy count rate for the first two PCs. Fig. 6 displays each depth spectrum in the new coordinate system projected onto the first two PCs. Separate spectral regions can be visually identified as being separate to one another. The three regions show: (1) the x-ray (2) the scatter and (3) the γ-photopeak.

The angle between PC1 to PC2 for model C is defined as θ in (3),

$$\theta = \tan^{-1}\left(\frac{PC2}{PC1}\right) \qquad (3)$$

where *PC1* is the first principal component and *PC2* is the second principal component.

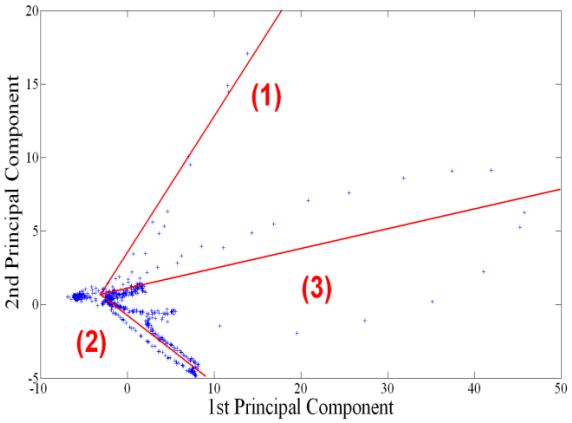

Fig. 6. The spectra projected onto PC1 and PC2 for model (C), the PCA computes the spectra to have mean zero. Region (1) relates to the x-ray, (2) the scatter and (3) the γ-photopeak.

Fig. 7 shows the dependence of θ with depth, and linear least-squares fit has been applied to it.

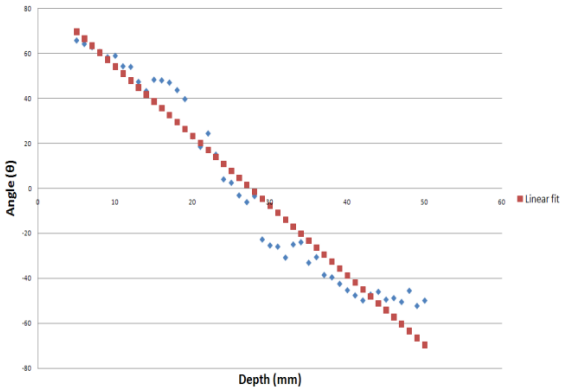

Fig. 7. The angle (θ) between the PC1 and PC2 vectors versus depth with linear least-squares fit.

It is evident from the data in fig. 7 that a non-linear dependence is more likely to describe the dependence of θ with depth. This is shown in fig. 8, however the resulting function was found to be too complex for use in the field to first order.

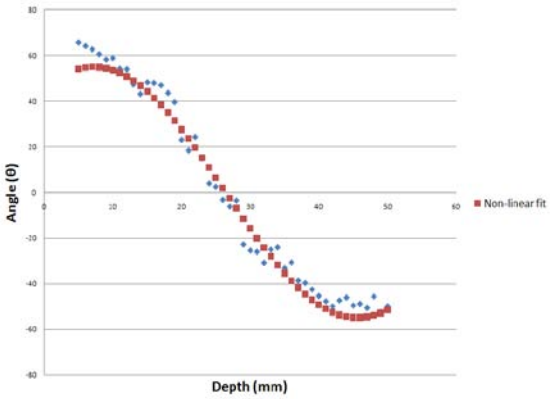

Fig. 8. The nonlinear fit between the angle (θ) and the depth.

IV. DISCUSSION

Using PCA on complete γ-ray spectra for a caesium-137 source buried under sand has enabled a linear relationship between the angle (θ) of the principal component vectors and the depth to be derived (4). Model C, incorporating the complete γ-ray spectra, provided the most accurate fit. Models (A & B) produced similar results, but were less accurate at lower depths. The results indicate that including the x-ray in the PCA model increases accuracy of the technique for sand depths <20mm.

A linear expression (4) for depth d as a function of angle θ, has been established from the data in fig. 7,

$$d = \frac{\theta - \beta}{\alpha} \qquad (4)$$

where α and β are constants. For Model C explored in this research α=-3.10±0.01 and β=85.1±0.2. A nonlinear fit has also been established which provides a better fit to the data but the linear relationship is most likely to be sufficient for practical use in the field.

The next stage of this research will be to test the PCA technique under greater shielding depths >50mm, and when using non-uniform grain sizes. This will be achieved by utilizing a bespoke 1m^3 soil phantom, enabling source depths to be investigated of up to 1m.

ACKNOWLEDGMENTS

The authors thank Alan Shippen for useful discussions and advice on sand phantoms, and Mark Salisbury for his assistance in constructing the source slider. Both are members of the Engineering Department at Lancaster University. This research is sponsored by REACT Engineering Ltd., the Engineering and Physical Sciences Research Council

(EPSRC) and the North West Development Agency (NWDA).

REFERENCES

[1] REACT Engineering Ltd, “Stop guessing…start predicting,” [Online]. Available: http://www.react-engineering.co.uk/n-visage.html

[2] A. Shippen and M.J. Joyce, “Profiling the depth of caesium-137 contamination in concrete via a relative linear attenuation model,” *Applied Radiation and Isotopes*., vol.68, no.4-5, pp.631-634, Apr-May.2010.

[3] Di-Yuan. Tzeng and Roy.S. Burns, “A Review of Principal Component Analysis and Its Applications to Color Technology,” *Color Research & Application*., vol.30, no.2, pp.84-98, Jan.2005.

[4] B.A. Shippen and M.J. Joyce, “The design and calibration of a phantom for depth profiling measurements of entrained radioactivity in silica-based media (Accepted for publication),” Nuclear Engineering and Design, (2010).

[5] *XRF corporation, " ICS-4000 Radionuclide Identifier" [Online]*. *Available:* http://www.xrfcorp.com/products/ics-4000.html.

[6] G. Gilmore and J. Hemingway, “Practical gamma-ray spectrometry,” Wiley, 1995.